# Local configurations in discrete combinatorial surfaces

Yukiko Kenmochi, Yusuke Nomura

# Local Configurations in Discrete Combinatorial Surfaces

Yukiko Kenmochi [a,*] Yusuke Nomura [b]

[a] *Institut Gaspard-Monge, Unité Mixte de Recherche CNRS-UMLV-ESIEE*
*Laboratoire A2SI, Groupe ESIEE*
*Cité Descartes, BP99, 93162 Noisy-le-Grand Cedex, France*

[b] *Department of Information Technology, Okayama University*
*3-1-1 Tsushimanaka, 700-8530 Okayama, Japan*

**Abstract**

Representing discrete objects by polyhedral complexes, we can define all conceivable topological characteristics of points in discrete objects, namely those of vertices of polyhedral complexes. Such a topological characteristic is determined for each point by observing a configuration of object points in the $3 \times 3 \times 3$ local point set of its neighbors. We study a topological characteristic such that the point is in the boundary of a 3D polyhedral complex and the boundary forms a 2D combinatorial surface. By using the topological characteristic, we present an algorithm which examines whether the central point of a local point set is in a combinatorial surface, and show how many local point configurations exist in combinatorial surfaces in a 3D discrete space.

*Key words:* discrete surface, local configurations, polyhedral complex

## 1 Introduction

Surfaces are often used in the three-dimensional image analysis, sometimes implicitly. For example, the method called active balloon uses a deformable surface for the three-dimensional image segmentation [5]. For such image segmentation, first an initial surface is set and then its shape is changed by using geometric characteristics such as curvatures. In many cases, such a deformable surface is realized by a continuous surface which is interpolated from discrete points in a three-dimensional digital space, such as a spline surface, and its

* Corresponding author. E-mail address: y.kenmochi@esiee.fr (Y. Kenmochi).

shape is changed by moving its control points in a continuous space [17]. If we need a result such as a segmented object in a discrete space after its continuous deformation, we therefore rediscretize the continuous surface to obtain a discrete object in a digital image. Obviously, continuous surface models are not efficient for the case such that both input and output are required to be discrete. It is more efficient to use a discrete surface model which allows us to make discrete deformation [7]. In this paper, we study discrete combinatorial surfaces and their local configurations, especially in the $3 \times 3 \times 3$ point region. We insist that such local configurations determine local geometric parameters such as curvatures in a discrete space. Therefore, if we can obtain all local configurations appearing in discrete surfaces a priori, we can expect to obtain useful properties which may give us efficient algorithms for calculation of geometric parameters as well as those for surface deformation based on such parameters.

Let us consider a three-dimensional discrete space $\mathbb{Z}^3$, consisting of lattice points whose coordinates are all integers in a three-dimensional Euclidean space $\mathbb{R}^3$. In our previous work [14], we presented a boundary extraction algorithm which provides a triangulation (or polygonization) of a set of boundary points given by

$$Br_m(\mathbf{V}) = \{\boldsymbol{x} \in \mathbf{V} : \mathbf{N}_m(\boldsymbol{x}) \cap \overline{\mathbf{V}} \neq \emptyset\} \tag{1}$$

where $\mathbf{V}$ is the input, i.e., a discrete object in $\mathbb{Z}^3$ and $\overline{\mathbf{V}}$ is the complement. $\mathbf{N}_m(\boldsymbol{x})$ is the $m$-neighborhood of a point $\boldsymbol{x}$ in $\mathbb{Z}^3$, defined by

$$\mathbf{N}_m(\boldsymbol{x}) = \{\boldsymbol{y} \in \mathbb{Z}^3 : \|\boldsymbol{x} - \boldsymbol{y}\|^2 \leq t\}$$

where $t = 1, 2, 3$ for $m = 6, 18, 26$ respectively. Applying discrete polyhedral complexes [14] based on combinatorial topology [1,19,20] to object representation, we can obtain topologies for boundary points. With a help of the topologies, we found that boundary points in $Br_m(\mathbf{V})$ include not only surface points, i.e., points on 2-dimensional combinatorial manifolds, but also non-surface points, i.e., singular points, as shown in Fig. 1. In this paper, we use local topological notions similarly to our work [12] to discriminate surface

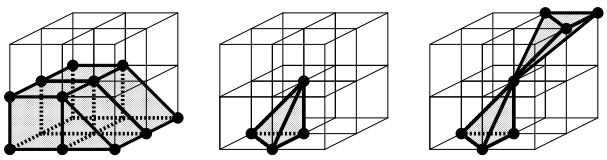

Fig. 1. Examples of local configurations in a $3 \times 3 \times 3$ point region so that the central point is considered to be a boundary point [14]; a surface point (left), a surface point but not a simplicity surface point [6] (center), and a non-surface point, i.e., a singular point (right).

points from boundary points. Such notions enable us to present an algorithm to count the local point configurations appearing in discrete combinatorial surfaces for the 6-, 18- and 26-neighborhood systems; discrete combinatorial surfaces are defined for any $m$-neighborhood system, $m = 6, 18, 26$, such that their adjacent vertices are $m$-neighboring. Because there are a finite number of points in the local region, there must be a finite number of local point configurations in discrete combinatorial surfaces.

For the 6-neighborhood system, the definition of discrete combinatorial surfaces is given by Françon in [8] and he showed that there are 6 local configurations of discrete surfaces for the 6-neighborhood system as illustrated in Fig. 2. Note that the similar results are obtained by using different approaches, for example, in [10,11]. The discrete deformation model based on such discrete surface configurations for 6-neighborhood system is also presented in [7]. Moreover, Françon and Kenmochi *et al.* show that there are five local configurations which appear in discrete planes, illustrated as the five left configurations in Fig. 2 [9,13]. In other words, there is only one configuration (the most right one in Fig. 2) which does not appear in discrete planes but appears in discrete non-planar surfaces.

In [8], however, the 18- and 26-neighborhoods are not practically treated so that we do not see how to generate discrete combinatorial surfaces for the 18- and 26-neighborhood systems, even if the mathematical definition is given for any neighborhood system. Morgenthaler *et al.* defined discrete surfaces by using the point connectivity based on the Jordan surface theorem; any Jordan surface divides the space into two [18]. In [6], Couprie *et al.* pointed out that, for the 26-neighborhood system, Morgenthaler's discrete surfaces have only 13 local configurations while their discrete surfaces, called simplicity surfaces, have 736 configurations. However, we see that even simplicity surfaces do not give enough configurations if we would like to treat our boundary points. For example, we obtain a boundary point by applying our boundary extraction algorithm [14] as illustrated in Fig. 1 (center) and we see that it is not considered to be a simplicity surface. Ciria *et al.* also presented a graph-based notion of discrete surfaces for the 26-neighborhood system, though the number of all local point configurations has not been studied yet [4].

To tackle the problem above, we take the approach based on polyhedral complexes similarly to our previous work [13,14]. The organization of our pa-

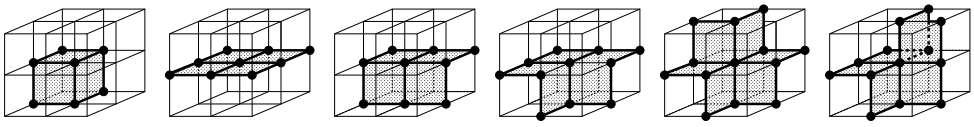

Fig. 2. The 6 local configurations of discrete combinatorial surfaces for the 6-neighborhood system [8,10,11] where the five left ones appears in discrete planes [9,13].

per is as follows. In Section 2, we first define discrete polyhedral complexes [14], based on combinatorial topology [1,19,20], which gives a topology to a three-dimensional discrete space. In Section 3, we then study topological characteristics of discrete polyhedral complexes similarly to [12]. By using these topological characteristics, in Section 4, we consider all conceivable topological characteristics of object points and distinguish those of boundary points such that the boundary forms a discrete combinatorial surface. After presenting an algorithm to examine whether a local point set forms a discrete combinatorial surface, we count local point configurations in discrete combinatorial surfaces, called local surface configurations, for each neighborhood system in Section 5. Finally, we show that such local surface configurations for the 6-neighborhood system are the same 6 ones as illustrated in Fig. 2 and derive new results for the 18- and 26-neighborhood systems. We also discuss the utilities of such study on local configurations in discrete surfaces for three-dimensional shape analysis in Section 6. This paper is an extended version of [15].

## 2 Discrete polyhedral complexes

In combinatorial topology, any object in $\mathbb{R}^3$ is represented by a set of simplexes [1,19] or more generally polyhedra [1,20]. An $n$-dimensional simplex is considered to be an $n$-dimensional element in $\mathbb{R}^3$ where $n$ can be from 0 to 3; 0-, 1-, 2- and 3-dimensional simplexes are defined as isolated points, line segments, triangles, and tetrahedra, respectively. A set of simplexes which are combined together without contradiction is called a complex [1,19]. Replacing simplexes with convex polyhedra, we obtain polyhedral complexes [1,20] instead of simplicial complexes.

In this paper, we construct convex polyhedra whose vertices are lattice points in $\mathbb{Z}^3$ and adjacent vertices are $m$-neighboring for $m = 6, 18, 26$. Such convex polyhedra are called discrete convex polyhedra, and a discrete polyhedral complex is constructed as a set of discrete convex polyhedra combined together without contradiction [14].

### *2.1 Convex polyhedra and polyhedral complexes in* $\mathbb{R}^3$

For the definitions of convex polyhedra and polyhedral complexes in $\mathbb{R}^3$, we follow the notions in [20]. Similar notations are also seen in [1,19].

**Definition 1** *A convex polyhedron $\sigma$ is the convex hull of a finite set of points in some $\mathbb{R}^n$.*

The dimension of a convex polyhedron $\sigma$ is the dimension of its hull. An $n$-dimensional convex polyhedron $\sigma$ is abbreviated to an $n$-polyhedron. For instance, a point is a 0-polyhedron, a line segment is a 1-polyhedron, a triangle or a square is a 2-polyhedron, and a tetrahedron or a hexahedron is a 3-polyhedron.

**Definition 2** *Let $\sigma$ be an $n$-polyhedron. A linear inequality $\boldsymbol{a} \cdot \boldsymbol{x} \leq z$ is said to be valid for $\sigma$ if it is satisfied for all points $\boldsymbol{x} \in \sigma$. A face of $\sigma$ is defined by any set of the form*

$$\delta = \sigma \cap \{\boldsymbol{x} \in \mathbb{R}^3 : \boldsymbol{a} \cdot \boldsymbol{x} = z\}$$

*where $\boldsymbol{a} \cdot \boldsymbol{x} \leq z$ is valid for $\sigma$.*

For instance, a 3-polyhedron which is a tetrahedron has four 0-polyhedra, six 1-polyhedra and four 2-polyhedra for its faces. If an $n$-polyhedron $\tau$ is a face of $\sigma$, $\tau$ is called an $n$-face and such a binary relation is denoted by $\tau \prec \sigma$.

The point of a 0-polyhedron, the endpoints of a 1-polyhedron and the vertices of 2- and 3-polyhedra are called the vertices of each convex polyhedron.

**Definition 3** *A polyhedral complex $\mathbf{C}$ is a finite collection of convex polyhedra such that*

*(1) the empty polyhedron is in $\mathbf{C}$,*
*(2) if $\sigma \in \mathbf{C}$ and $\tau \prec \sigma$, then $\tau \in \mathbf{C}$,*
*(3) if $\sigma, \tau \in \mathbf{C}$, then the intersection $\sigma \cap \tau$ is a common face of $\sigma$ and $\tau$.*

The dimension of $\mathbf{C}$ is the largest dimension of a convex polyhedron in $\mathbf{C}$.

We see that any $\mathbf{C}$ is a partially ordered set which can be identified with a topological space called a discrete space; the detail is found in Section 6 of Chapter 1 in [1].

### *2.2 Discrete convex polyhedra*

We consider discrete polyhedral complexes which are polyhedral complexes such that vertices of convex polyhedra are all lattice points in $\mathbb{Z}^3$ and adjacent vertices are $m$-neighboring for $m = 6, 18, 26$. The constraints allow us to look for a discrete convex polyhedron which is not larger than the unit cubic region as follows. The explication is also found in [14].

Let us consider all possible convex polyhedra in a unit cubic region such that the vertices of each convex polyhedron are vertices of a unit cube. A unit cube

Table 1
All possible discrete convex polyhedra for the 6-, 18- and 26-neighborhood systems.

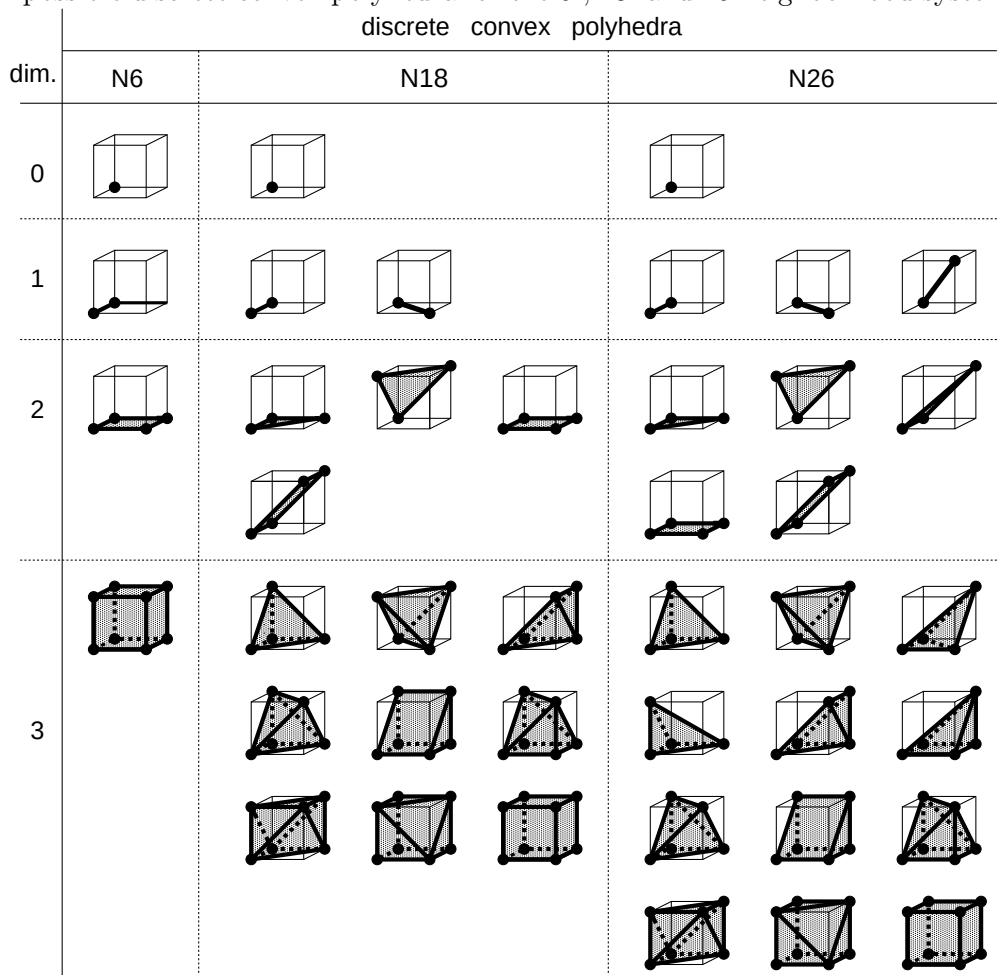


has eight lattice points for its vertices. For each lattice point we assign the value of either 1 or 0 and call the point a 1- or 0-point, respectively. We then obtain $2^8$ different 1-point configurations in a unit cube and, up to rotations and symmetries, we can reduce the number of different configurations to 22. Note that, among the 22 configurations, there are 21 configurations including at least one 1-point. For each of the 21 configurations, we obtain a convex polyhedron such that vertices of the polyhedron are 1-points. We then classify the 21 convex polyhedra with the dimension of $n = 0, 1, 2, 3$ and with the $m$-neighboring relations of adjacent vertices for $m = 6, 18, 26$ as shown in Table 1. We see that all 21 convex polyhedra are classified for $m = 26$ and parts of them are classified for $m = 6, 18$.

For any neighborhood system, 0-dimensional discrete convex polyhedra are isolated points. For 1-, 2- and 3-dimensional discrete convex polyhedra, in the case of the 6-neighborhood, the distance between any adjacent vertices is equal to 1, and in the case of the 26-neighborhood, it is equal to or less than $\sqrt{3}$. Hereafter, we abbreviate $n$-dimensional discrete convex polyhedra

to $n$-dimensional discrete polyhedra or simply $n$-polyhedra.

### *2.3 Discrete polyhedral complexes*

We construct a discrete polyhedral complex which is a finite collection of discrete convex polyhedra satisfying the three conditions in Definition 3 for each $m$-neighborhood system. In this paper, we need to construct a discrete polyhedral complex only in the local region such as $3 \times 3 \times 3$. Even though we present an algorithm for construction of a discrete polyhedral complex in such a local region in this subsection, we remark that the same algorithm can be applied to three-dimensional binary images of various sizes. Mathematical details for obtaining discrete polyhedral complexes are found in [14].

Let us consider a point $\boldsymbol{x} \in \mathbb{Z}^3$ and the $3 \times 3 \times 3$ point region around $\boldsymbol{x}$, that is $\mathbf{N}_{26}(\boldsymbol{x})$. Given a subset $\mathbf{V} \subseteq \mathbf{N}_{26}(\boldsymbol{x})$, we explain how to construct a discrete polyhedral complex $\mathbf{C}_m$ for $m = 6, 18, 26$ from $\mathbf{V}$ in this subsection. We first consider the case of the 26-neighborhood, and then show how to modify our algorithm for the 18-neighborhood. For the 6-neighborhood, we refer to another method which is simple for constructing $\mathbf{C}_6$ from $\mathbf{V}$.

Hereafter, we abbreviate an $n$-dimensional discrete polyhedral complex to an $n$-dimensional discrete complex or simply an $n$-complex.

#### *2.3.1 Discrete complex construction for the 26-neighborhood system*

We first consider a $2 \times 2 \times 2$ unit cubic region which is a set of eight lattice points for any $\boldsymbol{x} = (p, q, r)$ in $\mathbb{Z}^3$ such that

$$\mathbf{D}(\boldsymbol{x}) = \{p, p+1\} \times \{q, q+1\} \times \{r, r+1\}.$$

Obviously, $\mathbf{D}(\boldsymbol{x})$ includes $\boldsymbol{x}$ itself. Therefore, any $3 \times 3 \times 3$ point region $\mathbf{N}_{26}(\boldsymbol{x})$ is divided into eight unit cubic regions $\mathbf{D}(\boldsymbol{y})$ such that

$$\mathbf{N}_{26}(\boldsymbol{x}) = \bigcup_{\boldsymbol{y} \in \mathbf{W}(\boldsymbol{x})} \mathbf{D}(\boldsymbol{y})$$

where $\mathbf{W}(\boldsymbol{x}) = \mathbf{D}(\boldsymbol{x} - (1, 1, 1))$.

All points in $\mathbf{V}$ (resp. the complement $\overline{\mathbf{V}}$) are 1-points (resp. 0-points). Setting the set of 1-points in a unit cube $\mathbf{D}(\boldsymbol{y})$ as

$$\mathbf{U}(\boldsymbol{y}) = \mathbf{D}(\boldsymbol{y}) \cap \mathbf{V},$$

we first construct a discrete complex from $\mathbf{U}(\boldsymbol{y})$ in a unit cube $\mathbf{D}(\boldsymbol{y})$, denoted by $cmp_{26}(\mathbf{U}(\boldsymbol{y}))$. We then obtain a discrete complex $\mathbf{C}_{26}$ with respect to $\mathbf{V}$, which is also denoted by $cmp_{26}(\mathbf{V})$, such that

$$\mathbf{C}_{26} = \bigcup_{\boldsymbol{y} \in \mathbf{W}(\boldsymbol{x})} cmp_{26}(\mathbf{U}(\boldsymbol{y})) \tag{2}$$

for $\boldsymbol{x}$ is the central point in $\mathbf{N}_{26}(\boldsymbol{x})$. In [14], mathematical proof of (2) is given.

A discrete complex $cmp_{26}(\mathbf{U}(\boldsymbol{y}))$ is constructed from $\mathbf{U}(\boldsymbol{y})$ by the following algorithm. Let $\mathbf{P}_n$ be a set of $n$-polyhedra in $cmp_{26}(\mathbf{U}(\boldsymbol{y}))$ for $n = 0, 1, 2, 3$. Note that $|\mathbf{A}|$ denotes the number of elements of a set $\mathbf{A}$ and that $Ver(\sigma)$ denotes a set of 0-faces (or lattice points) of an $n$-polyhedron $\sigma$, namely vertices of $\sigma$.

**Algorithm 1**

***Input:*** *A 1-point set* $\mathbf{U}(\boldsymbol{y})$ *in a unit cubic region* $\mathbf{D}(\boldsymbol{y})$.
***Output:*** *A discrete complex* $cmp_{26}(\mathbf{U}(\boldsymbol{y}))$.
***begin***

*1* **if** $|\mathbf{U}(\boldsymbol{y})| \geq 5$, **then** *create a 3-polyhedron as a convex hull of all points in* $\mathbf{U}(\boldsymbol{y})$ *and put it in* $\mathbf{P}_3$*;*

*2* **else if** $|\mathbf{U}(\boldsymbol{y})| = 4$ *and the four points are not coplanar,* **then** *create a 3-polyhedron as a convex hull of all points in* $\mathbf{U}(\boldsymbol{y})$ *and put it in* $\mathbf{P}_3$*;*

*3* **else if** $|\mathbf{U}(\boldsymbol{y})| = 4$ *and the four points are coplanar,* **then** *create a 2-polyhedron as a convex hull of all points in* $\mathbf{U}(\boldsymbol{y})$ *and put it in* $\mathbf{P}_2$*;*

*4* **else if** $|\mathbf{U}(\boldsymbol{y})| = 3$, **then** *create a 2-polyhedron as a convex hull of all points in* $\mathbf{U}(\boldsymbol{y})$ *and put it in* $\mathbf{P}_2$*;*

*5* **else if** $|\mathbf{U}(\boldsymbol{y})| = 2$, **then** *create a 1-polyhedron as a convex hull of all points in* $\mathbf{U}(\boldsymbol{y})$ *and put it in* $\mathbf{P}_1$*;*

*6* **for each** *3-polyhedron* $\sigma \in \mathbf{P}_3$*, look for all 2-faces* $\tau$ *of* $\sigma$ *such that* $Ver(\tau)$ *is a three- or four-point subset of* $Ver(\sigma)$ *where all points in* $Ver(\tau)$ *are coplanar and all points in* $Ver(\sigma) \setminus Ver(\tau)$ *are in one side of the plane spanned by points in* $Ver(\tau)$*, and put all such* $\tau$ *in* $\mathbf{P}_2$*;*

*7* **for each** *2-polyhedron* $\sigma \in \mathbf{P}_2$*,*

*7.1* **if** $|Ver(\sigma)| = 3$*, consider all 1-faces* $\tau$ *of* $\sigma$ *such that* $Ver(\tau)$ *is any two-point subset of* $Ver(\sigma)$*, and put all* $\tau$ *in* $\mathbf{P}_1$*;*

*7.2* **if** $|Ver(\sigma)| = 4$*, look for all 1-faces* $\tau$ *of* $\sigma$ *such that the distance between the two points of* $Ver(\tau)$ *is one, or such that the distance between the two points of* $Ver(\tau)$ *is* $\sqrt{2}$ *when there exist exactly two pairs of points whose distance is* 1 *in* $Ver(\sigma)$*, and put all such* $\tau$ *in* $\mathbf{P}_1$*;*

*8 set* $\mathbf{P}_0 = \{\{\boldsymbol{z}\} : \boldsymbol{z} \in \mathbf{U}(\boldsymbol{y})\}$*;*

*9 obtain* $cmp_{26}(\mathbf{U}(\boldsymbol{y})) = \bigcup_{n=0,1,2,3} \mathbf{P}_n$.

***end***

Table 2
Five 1-point configurations of a unit cube where different discrete complexes are constructed for the 18- and 26-neighborhood systems.

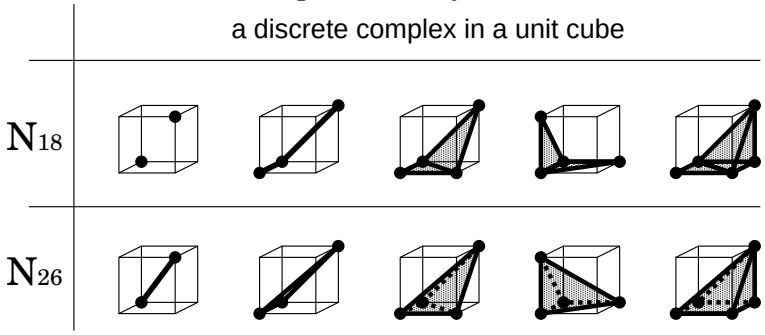


In Steps 6 (resp. 7), we also store binary relations $\prec$ between 3- and 2-polyhedra (resp. 2- and 1-polyhedra).

### *2.3.2 Discrete complex construction for the* 18*-neighborhood system*

Let us consider the case of $m = 18$. The right column of Table 1 shows that there are 22 different 1-point configurations of a unit cube for discrete complex construction in the case that $m = 26$. It also shows that there are five 1-point configurations missing for the 18-neighborhood system in comparison with those for the 26-neighborhood system. This is because each of those five convex polyhedra includes a pair of adjacent vertices which are 26-neighboring but not 18-neighboring. Therefore, to construct a discrete complex in a unit cube whose 1-point configuration is one of those five for the 18-neighborhood system, we cannot apply Algorithm 1. Table 2 illustrates the discrete complexes expected for the 18-neighborhood, which are different from those for the 26-neighborhood.

In order to obtain each discrete complex in the first line of Table 2, we first decompose a unit cube into two cubes as shown in Table 3. We then apply Algorithm 1 for each unit cube except for the following exceptional cases.

Let us consider a unit cube $\mathbf{D}(\boldsymbol{y})$ which is the last case in Table 3. At an adjacent cube $\mathbf{D}(\boldsymbol{z})$ which shares four 1-points with $\mathbf{D}(\boldsymbol{y})$, we need to modify its polyhedral complex $cmp_{18}(\mathbf{U}(\boldsymbol{z}))$. Figure 3 illustrates that if $cmp_{18}(\mathbf{U}(\boldsymbol{z}))$ has a squared 2-polyhedron $\sigma$ whose vertices are the four shared 1-points, we must replace $\sigma$ with two triangle 2-polyhedra $\tau_1$, $\tau_2$ and their common face $\tau_3$ which is a 1-polyhedron, such that $cmp_{18}(\mathbf{U}(\boldsymbol{z})) \setminus \{\sigma\} \cup \{\tau_1, \tau_2, \tau_3\}$. We remark that such a replacement does not destroy the topology of a discrete complex.

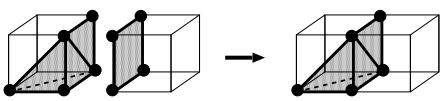

Fig. 3. Additional polyhedral decomposition for the 18-neighborhood system.

Table 3
Each unit cube in Table 2 is decomposed into two unit cubes for discrete complex construction in the case of the 18-neighborhood system.

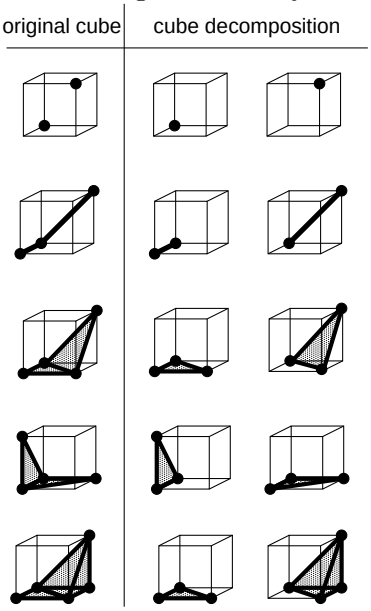


Table 4
A unit cube of the last line in Table 3 is decomposed into three unit cubes for discrete complex construction in the case of the 18-neighborhood system, if unit cubes are adjacent as illustrated in Fig. 4 (left).

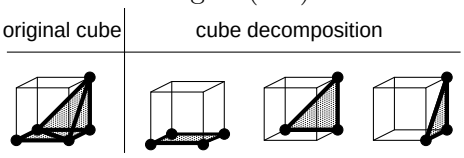


If an adjacent cube $\mathbf{D}(\boldsymbol{z})$ also has the last configuration in Table 3, that is, both $\mathbf{D}(\boldsymbol{y})$ and $\mathbf{D}(\boldsymbol{z})$ have the last 1-point configuration in Table 3 and they share four 1-points, and if the distance between two 1-points which are not shared by $\mathbf{D}(\boldsymbol{y})$ and $\mathbf{D}(\boldsymbol{z})$ is $\sqrt{5}$, as illustrated in the left figure of Fig. 4, we modify the polyhedral complexes in both cubes, $cmp_{18}(\mathbf{U}(\boldsymbol{y}))$ and $cmp_{18}(\mathbf{U}(\boldsymbol{z}))$, as illustrated in the right figure of Fig. 4. For such a modification, we decompose each unit cube of $\mathbf{D}(\boldsymbol{y})$ and $\mathbf{D}(\boldsymbol{z})$ into three unit cubes as shown in Table 4 before applying Algorithm 1 at each unit cube.

We remark that the modification of polyhedral complexes as illustrated in

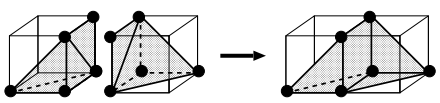

Fig. 4. Modification of polyhedral complexes in two adjacent unit cubes such that each of them has the last 1-point configuration in Table 3, and they have four common 1-points and also have two non-common 1-points whose distance is $\sqrt{5}$, for the 18-neighborhood system.

Fig. 4 causes the problem such that a discrete complex $\mathbf{C}_{18}$ constructed from $\mathbf{V} \subseteq \mathbf{N}_{26}(\boldsymbol{x})$ does not depend only on the $3 \times 3 \times 3$ point region, namely $\mathbf{N}_{26}(\boldsymbol{x})$, when $\boldsymbol{x}$ is the leftmost (or rightmost) point in Fig. 4. We will discuss how we deal with this problem for topological classification of local point configurations at the end of Section 4.

### *2.3.3 Discrete complex construction for the 6-neighborhood system*

In order to construct a discrete complex $\mathbf{C}_6$ from a 1-point set $\mathbf{V}$, we can have a geometric algorithm similar to Algorithm 1 which is applied at each unit cube $\mathbf{D}(\boldsymbol{y})$ to construct $cmp_6(\mathbf{U}(\boldsymbol{y}))$ and then obtain $\mathbf{C}_6$ by (2). However, it is more efficient to apply a method to construct a Khalimsky topology [16] or a partially order set associated to $\mathbb{Z}^n$ [2,3]; our discrete polyhedral complex for the 6-neighborhood system is equivalent to the above partially order set and it gives a topology equivalent to a Khalimsky topology. In [2] it is mentioned that a three-dimensional array whose size is $5 \times 5 \times 5$ is used for storing such a topology for a $3 \times 3 \times 3$ local point set.

## *2.4 Properties of discrete polyhedral complexes*

We will present several properties of discrete complexes which we will need in the following sections.

**Definition 4** *Let* $\mathbf{C}$ *be an* $n$*-complex. If we have at least one* $n$*-polyhedron* $\sigma \in \mathbf{C}$ *for every* $s$*-polyhedron* $\tau \in \mathbf{C}$ *such that* $\tau \prec \sigma$, $\mathbf{C}$ *is said to be pure.*

Figure 5 shows examples of pure and non-pure discrete complexes. The 3-complex in Fig. 5 (a) is not pure because it includes 0-, 1- and 2-polyhedra which do not belong to any 3-polyhedron. If we remove these 0-, 1- and 2-polyhedra from Fig. 5 (a), we obtain a pure 3-complex in Fig. 5 (b).

We need the following notion of combinatorial closure to obtain a discrete complex from a set of discrete polyhedra, and by using this notion we present the connectivity of a discrete complex.

**Definition 5** *Let* $\mathbf{C}$ *be a discrete complex and* $\mathbf{B}$ *be a subset of* $\mathbf{C}$*. The com-*

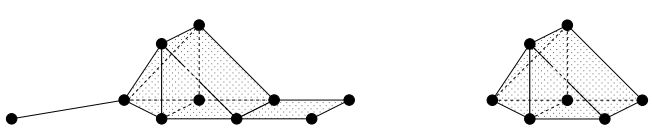

(a) (b)

Fig. 5. (a) Non-pure and (b) pure 3-complexes.

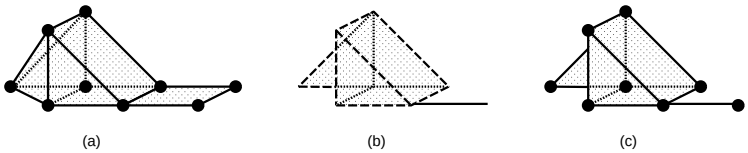


Fig. 6. (a) A 3-complex $\mathbf{C}$, (b) its subset $\mathbf{B}$ consisting of three convex polyhedra whose dimensions are from one to three respectively, and (c) the closure of $\mathbf{B}$ in $\mathbf{C}$.

*binatorial closure of* $\mathbf{B}$ *is defined as*

$$Cl(\mathbf{B}) = \mathbf{B} \cup \{\tau \in \mathbf{C} : \tau \prec \sigma,\ \sigma \in \mathbf{B}\}.$$

Note that $\mathbf{B}$ may not be a complex while $Cl(\mathbf{B})$ is always a complex, and $\mathbf{B} \neq Cl(\mathbf{B})$ if $\mathbf{B}$ is not a complex. Figure 6 shows an example of the closure of a subset for a given complex.

**Definition 6** *Let* $\mathbf{C}$ *be a discrete complex, and* $\sigma, \tau$ *be arbitrary elements in* $\mathbf{C}$*. We say that* $\mathbf{C}$ *is connected, if we have a path* $\sigma = a_1, a_2, \ldots, \tau = a_n$ *which satisfies the following conditions:*

*(1)* $a_i \in \mathbf{C}$ *for every* $i = 1, 2, \ldots, n$*;*
*(2)* $Cl(\{a_i\}) \cap Cl(\{a_{i+1}\}) \neq \emptyset$ *for every* $i = 1, 2, \ldots, n-1$*.*

## 3 Topological point characterization on discrete complexes

Let $Sk(\mathbf{C})$ be the union of all 0-polyhedra in a discrete complex $\mathbf{C}$, namely the union of $Ver(\sigma)$ for all discrete convex polyhedra $\sigma \in \mathbf{C}$, called the skeleton of $\mathbf{C}$. Obviously, $Sk(\mathbf{C}) = \mathbf{V}$ if $\mathbf{C}$ is made from $\mathbf{V}$.

The goal of this paper is to present an algorithm to verify whether each point in $Sk(\mathbf{C})$ is considered to be on a discrete surface or not. For that goal, we study topological characterization of each point in $Sk(\mathbf{C})$ by observing its local point configuration and investigate all topological characteristics which can be maintained by points in $Sk(\mathbf{C})$. In $\mathbb{Z}^3$, we have discrete complexes whose dimensions can be from zero to three. Thus, we present topological characterization of discrete complexes for each dimension from one to three by using the notions of star and link [20] similarly to the previous work [12]. We then show that there are 12 topological types of points in $Sk(\mathbf{C})$. In the next sections, we will classify all points in $Sk(\mathbf{C})$ by their topological characteristics and study the type of points in discrete surfaces.

In this section, we do not have to distinguish the three different neighborhood systems. Thus, we abbreviate a discrete complex $\mathbf{C}_m$ for $m = 6, 18, 28$ simply to $\mathbf{C}$.

### *3.1 Star and link*

The star and the link are defined for each point in $Sk(\mathbf{C})$ as follows.

**Definition 7** *For a discrete complex* $\mathbf{C}$*, the star of a point* $\boldsymbol{x} \in Sk(\mathbf{C})$ *is defined such that*

$$star(\boldsymbol{x}) = \{\sigma \in \mathbf{C} : \boldsymbol{x} \in \sigma\}.$$

**Definition 8** *For a discrete complex* $\mathbf{C}$*, the link of a point* $\boldsymbol{x} \in Sk(\mathbf{C})$ *is defined such that*

$$link(\boldsymbol{x}) = Cl(star(\boldsymbol{x})) \setminus star(\boldsymbol{x}).$$

The star and link with respect to $\mathbf{C}$ are denoted by $star(\boldsymbol{x} : \mathbf{C})$ and $link(\boldsymbol{x} : \mathbf{C})$, respectively, when we emphasize $\mathbf{C}$.

The star is defined with respect to a point $\boldsymbol{x}$ in $Sk(\mathbf{C})$ as the set of discrete convex polyhedra including $\boldsymbol{x}$. For example, let us consider the star of a point $\boldsymbol{x}$ in Fig. 7 (a). It includes, as shown in Fig. 7 (b), a pentahedral 3-polyhedron, four triangle 2-polyhedra, four line-segment 1-polyhedra, and a 0-polyhedron which is the point $\boldsymbol{x}$ itself. The link of $\boldsymbol{x}$ in Fig. 7 (a) is obtained such as a squared 2-polyhedron and its faces as shown in Fig. 7 (c). Similarly to discrete complexes, we define the dimension of $star(\boldsymbol{x} : \mathbf{C})$ as the maximum dimension of discrete convex polyhedra belonging to $star(\boldsymbol{x} : \mathbf{C})$ and denoted by $dim(star(\boldsymbol{x} : \mathbf{C}))$. Note that a star is not always a discrete complex because it may not satisfy the second condition in Definition 3.

### *3.2 Topological characteristics of stars in one dimension*

Stars of points in $Sk(\mathbf{C})$ are classified into the following three types: linear stars, semi-linear stars, and neither of them, when the dimensions of stars are one.

**Definition 9** *Let* $\mathbf{C}$ *be a discrete complex and* $\boldsymbol{x}$ *be a point in* $Sk(\mathbf{C})$*. We say that* $star(\boldsymbol{x})$ *is linear if* $link(\boldsymbol{x})$ *consists of two* 0*-polyhedra.*

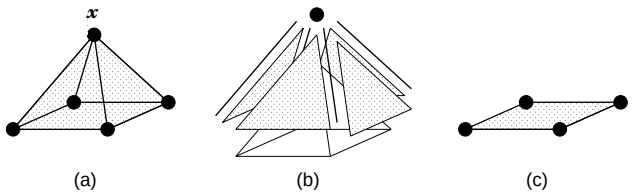


Fig. 7. (a) A 3-complex $\mathbf{C}$; (b) the star of $\boldsymbol{x} \in Sk(\mathbf{C})$; (c) the link of $\boldsymbol{x}$.

**Definition 10** *Let* $\mathbf{C}$ *be a discrete complex and* $\boldsymbol{x}$ *be a point in* $Sk(\mathbf{C})$*. We say that* $star(\boldsymbol{x})$ *is semi-linear if* $link(\boldsymbol{x})$ *consists of one* 0*-polyhedron.*

Figure 8 illustrates points whose stars are linear, semi-linear and neither of them. We see that a point is an endpoint of a curve if its star is semi-linear, and an intermediate point of a curve if its star is linear. If the star of a point is neither linear nor semi-linear, it is an intersection of a curve. By using the above definitions, we define discrete curves in $\mathbb{Z}^3$.

**Definition 11** *Let* $\mathbf{C}$ *be a connected and pure* 1*-complex. We say that* $\mathbf{C}$ *is a discrete curve with endpoint if the star of every point in* $Sk(\mathbf{C})$ *is either linear or semi-linear and there is at least one point whose star is semi-linear in* $Sk(\mathbf{C})$*.*

**Definition 12** *Let* $\mathbf{C}$ *be a connected and pure* 1*-complex. We say that* $\mathbf{C}$ *is a discrete closed curve if the star of every point in* $Sk(\mathbf{C})$ *is linear.*

### *3.3 Topological characteristics of stars in two dimensions*

Stars of points in $Sk(\mathbf{C})$ are classified into the following three types: cyclic stars, semi-cyclic stars, and neither of them, when the dimensions of stars are two.

**Definition 13** *Let* $\mathbf{C}$ *be a discrete complex and* $\boldsymbol{x}$ *be a point in* $Sk(\mathbf{C})$*. We say that* $star(\boldsymbol{x})$ *is cyclic if* $link(\boldsymbol{x})$ *is a discrete closed curve.*

**Definition 14** *Let* $\mathbf{C}$ *be a discrete complex and* $\boldsymbol{x}$ *be a point in* $Sk(\mathbf{C})$*. We say that* $star(\boldsymbol{x})$ *is semi-cyclic if* $link(\boldsymbol{x})$ *is a discrete curve with endpoint.*

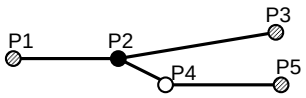


Fig. 8. Examples of points whose stars are linear, semi-linear and neither of them, illustrated as white, grey and black points, respectively.

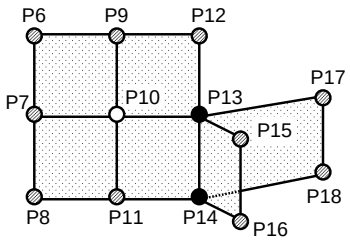


Fig. 9. Examples of points whose stars are cyclic, semi-cyclic, and neither of them, illustrated as white, grey and black points, respectively.

Figure 9 illustrates points of stars which are cyclic, semi-cyclic and neither of them. We see that a point is an edge point of a surface if its star is semi-cyclic, and an interior point of a surface if its star is cyclic. If the star of a point is neither cyclic nor semi-cyclic, the point is at an intersection of surfaces. By using these characteristics, we define discrete surfaces in $\mathbb{Z}^3$.

**Definition 15** *Let* $\mathbf{C}$ *be a connected and pure* 2*-complex. We say that* $\mathbf{C}$ *is a discrete surface with edge if every point in* $Sk(\mathbf{C})$ *has either a cyclic or semi-cyclic star, and there is at least one point whose star is semi-cyclic in* $Sk(\mathbf{C})$*.*

**Definition 16** *Let* $\mathbf{C}$ *be a connected and pure* 2*-complex. We say that* $\mathbf{C}$ *is a discrete closed surface if every point in* $Sk(\mathbf{C})$ *has a cyclic star.*

Definition 15 (resp. 16) is similar to the definition of a two-dimensional combinatorial manifold with (resp. without) boundary in reference [8]. In fact, the notion of cyclic stars in Definition 13 corresponds to that of umbrellas in [8].

### *3.4 Topological characteristics of stars in three dimensions*

Stars of points in $Sk(\mathbf{C})$ are classified into the following three types: spherical stars, semi-spherical stars, and neither of them, when the dimensions of stars are three.

**Definition 17** *Let* $\mathbf{C}$ *be a discrete complex and* $\boldsymbol{x}$ *be a point in* $Sk(\mathbf{C})$*. We say that* $star(\boldsymbol{x})$ *is spherical if* $link(\boldsymbol{x})$ *is a discrete closed surface.*

We define semi-spherical stars by using the notion of combinatorial boundary.

**Definition 18** *Let* $\mathbf{C}$ *be a pure* $n$*-complex and* $\mathbf{H}$ *be the set of all* $(n-1)$*-polyhedra in* $\mathbf{C}$ *each of which is a face of exactly one* $n$*-polyhedron in* $\mathbf{C}$*. The combinatorial boundary of* $\mathbf{C}$ *is then defined as a pure* $(n-1)$*-complex such*

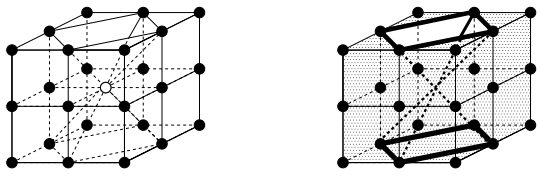

(a) (b)

Fig. 10. An example of a point whose star is considered to be semi-spherical with our previous definition in [12], but not semi-spherical with that in this paper, illustrated as the white point in (a). A halftone region and two black bold closed curves in (b) show its link and its combinatorial boundary.

*that*

$$\partial \mathbf{C} = Cl(\mathbf{H}).$$

We now see that the endpoints of a discrete curve and the edges of a discrete surface in Definitions 11 and 15 are their combinatorial boundaries. An example is shown in Fig. 10 (b). If we consider the link of the central white point in Fig. 10 (a) illustrated as a half-tone region in Fig. 10 (b), its combinatorial boundary is shown as black bold lines.

**Definition 19** *Let* $\mathbf{C}$ *be a discrete complex and* $\boldsymbol{x}$ *be a point in* $Sk(\mathbf{C})$*. We say that* $star(\boldsymbol{x})$ *is semi-spherical if* $link(\boldsymbol{x})$ *is a discrete surface with edge and the edge, i.e., the combinatorial boundary* $\partial(link(\boldsymbol{x}))$ *is a discrete closed curve.*

In the previous work [12], semi-spherical stars are simply defined such that $link(\boldsymbol{x})$ is a discrete surface with edges. However, we found a counter example such as a white central point in Fig. 10 (a); its link is a discrete surface with two boundaries, and its star should not be regarded as a semi-spherical star because it is not topologically equivalent to a semi-sphere. We therefore modify our definition of semi-spherical stars.

Figure 11 illustrates points whose stars are spherical, semi-spherical and neither of them. It also shows that a point whose star is spherical is an interior point in a 3-complex, a point whose star is semi-spherical is a boundary point of a 3-complex, and a point whose star is neither spherical nor semi-spherical is a singular point, i.e., an intersection point of the boundaries.

We present the following proposition which plays an important role in this paper.

**Proposition 20** *Let* $\mathbf{C}$ *be a pure* 3*-complex and* $\boldsymbol{x}$ *be a point in* $Sk(\mathbf{C})$*. If* $star(\boldsymbol{x} : \mathbf{C})$ *is semi-spherical, then* $star(\boldsymbol{x} : \partial\mathbf{C})$ *is cyclic.*

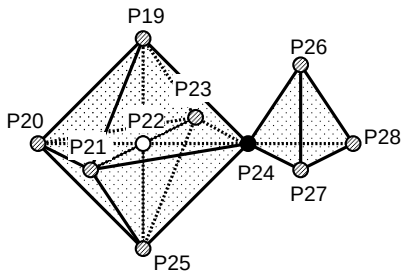


Fig. 11. Examples of points whose stars are spherical, semi-spherical and neither of them, illustrated as white, grey and black points, respectively.

**PROOF.** From Definition 19, $\partial(link(\boldsymbol{x} : \mathbf{C}))$ is a discrete closed curve. Let $\mathbf{H}$ be a set of all 1-polyhedra in $\partial(link(\boldsymbol{x} : \mathbf{C}))$ so that

$$\partial(link(\boldsymbol{x} : \mathbf{C})) = Cl(\mathbf{H}). \tag{3}$$

For any $\sigma \in \mathbf{H}$, from Definition 18, there is exactly one 2-polyhedron $\tau \in link(\boldsymbol{x} : \mathbf{C})$ such that $\sigma \prec \tau$. Therefore, for any $\sigma \in \mathbf{H}$, there is exactly one 3-polyhedron $\gamma \in star(\boldsymbol{x} : \mathbf{C})$ such that $\sigma \prec \gamma$ as well. We then easily see that $\sigma$ becomes the common 1-face of two 2-faces $\tau_1, \tau_2$ of $\gamma$. Because we know from the above that there is only one 2-face in $link(\boldsymbol{x} : \mathbf{C})$ for $\sigma$, set to be $\tau_1$, another 2-face $\tau_2$ is not in $link(\boldsymbol{x} : \mathbf{C})$ but in $star(\boldsymbol{x} : \mathbf{C})$. Such $\tau_2$ is a 2-face of exactly one 3-polyhedron in $star(\boldsymbol{x} : \mathbf{C})$, that is $\gamma$. Therefore, $\tau_2 \in star(\boldsymbol{x} : \partial\mathbf{C})$, and thus $\sigma \in Cl(star(\boldsymbol{x} : \partial\mathbf{C}))$ for any $\sigma \in \mathbf{H}$. Because $\sigma \notin star(\boldsymbol{x} : \partial\mathbf{C})$, we obtain

$$Cl(\mathbf{H}) = link(\boldsymbol{x} : \partial\mathbf{C}). \tag{4}$$

From (3) and (4), $link(\boldsymbol{x} : \partial\mathbf{C})$ becomes a discrete closed curve and consequently, $star(\boldsymbol{x} : \partial\mathbf{C})$ is cyclic from Definition 13.

### *3.5 Twelve point types by topological star characteristics*

By using topological characterization of stars described above, we classify points $\boldsymbol{x} \in Sk(\mathbf{C})$ into twelve types each of which satisfies one of the following conditions. Note that each point in $Sk(\mathbf{C})$ is classified into one of them.

**type 0:** $dim(star(\boldsymbol{x})) = 0$;
**type 1a:** $star(\boldsymbol{x})$ is linear;
**type 1b:** $star(\boldsymbol{x})$ is semi-linear;
**type 1c:** $dim(star(\boldsymbol{x})) = 1$ and $star(\boldsymbol{x})$ is neither linear nor semi-linear;
**type 2a:** $star(\boldsymbol{x})$ is cyclic;
**type 2b:** $star(\boldsymbol{x})$ is semi-cyclic;
**type 2c:** $dim(star(\boldsymbol{x})) = 2$, $Cl(star(\boldsymbol{x}))$ is pure and $star(\boldsymbol{x})$ is neither cyclic nor semi-cyclic;
**type 2d:** $dim(star(\boldsymbol{x})) = 2$ and $Cl(star(\boldsymbol{x}))$ is not pure;
**type 3a:** $star(\boldsymbol{x})$ is spherical;
**type 3b:** $star(\boldsymbol{x})$ is semi-spherical;
**type 3c:** $dim(star(\boldsymbol{x})) = 3$, $Cl(star(\boldsymbol{x}))$ is pure and $star(\boldsymbol{x})$ is neither spherical nor semi-spherical;
**type 3d:** $dim(star(\boldsymbol{x})) = 3$ and $Cl(star(\boldsymbol{x}))$ is not pure.

Some examples of points whose types are 2d and 3d are shown in Fig. 12.

Table 5
Classification results of points from P1 to P41 in Figs. 8, 9, 11, 12 (P1–P5 in Fig. 8, P6–P18 in Fig. 9, P19–P28 in Fig. 11, P29–P41 in Fig. 12 respectively) into the twelve types from 0 to 3d (no point for type 0).

| | classified points |
|---|---|
| **type 1a** | 4 |
| **type 1b** | 1, 3, 5, 33, 34 |
| **type 1c** | 2 |
| **type 2a** | 10 |
| **type 2b** | 6, 7, 8, 9, 11, 12, 15, 16, 17, 18, 29, 30, 31, 40, 41 |
| **type 2c** | 13, 14 |
| **type 2d** | 32 |
| **type 3a** | 22 |
| **type 3b** | 19, 20, 21, 23, 25, 26, 27, 28, 36, 37 |
| **type 3c** | 24 |
| **type 3d** | 35, 38, 39 |

Table 5 shows the classification results of all points from P1 to P41, illustrated in Figs. 8, 9, 11, 12, into the twelve types.

## 4 Topological classification of local point configurations

As we mentioned above, any point is classified into one of the twelve types. We also see that these twelve types have a hierarchical structure as shown in Fig. 13.

By using the hierarchical structure, we can easily obtain an algorithm to clas-

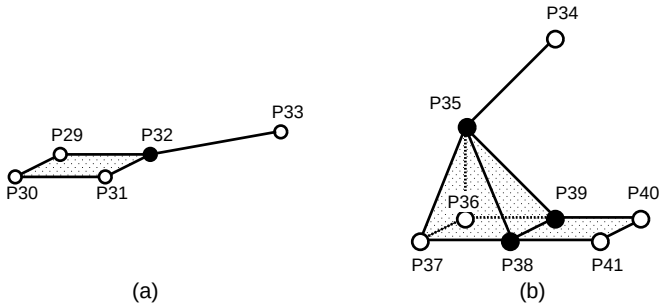


Fig. 12. Examples of points whose types are 2d (a) and 3d (b), shown as black points, in non-pure discrete complexes.

sify a local 1-point set $\mathbf{V}$ with respect to a type of the star of the central point $\boldsymbol{x} \in \mathbf{V}$:

(1) construct a discrete complex $\mathbf{C}_m$ for $m = 6, 18$ or 26 from $\mathbf{V}$;
(2) obtain $star(\boldsymbol{x})$ in $\mathbf{C}_m$;
(3) classify $star(\boldsymbol{x})$ by its dimension;
(4) if the dimension is more than zero, classify $star(\boldsymbol{x})$ by its topological characteristics (including the purity of $Cl(star(\boldsymbol{x}))$ for more than one dimension).

Note that $\boldsymbol{x}$ is always a 1-point for any 1-point configuration of $\mathbf{V}$. In addition, a discrete complex $\mathbf{C}_m$ for $m = 6, 18, 26$ is uniquely obtained from $\mathbf{V}$ as described in Section 2 mostly except for the case of $m = 18$ as mentioned at the end of Section 2.3.2. In order to simplify the situation for $m = 18$ and to obtain a unique type of the central point $\boldsymbol{x}$ for any input $\mathbf{V}$, we therefore assume that 1-points exist only in $\mathbf{N}_{26}(\boldsymbol{x})$ and there are only 0-points in the exterior. Consequently, if we have a unit cube which is the last case in Table 3 and whose four coplanar 1-points are located at the boundary of $\mathbf{N}_{26}(\boldsymbol{x})$ and shared by an adjacent unit cube in the exterior of $\mathbf{N}_{26}(\boldsymbol{x})$, the cube decomposition is simply considered as the last one of Table 3 but not as that of Table 4 to construct $\mathbf{C}_{18}$.

We apply the algorithm to every local 1-point configurations of $\mathbf{V} \subseteq \mathbf{N}_{26}(\boldsymbol{x})$ whose central point $\boldsymbol{x}$ is 1-point. The number of all possible 1-point configurations of $\mathbf{V}$ is $2^{26} = 67108864$, that is reduced to 1426144 up to rotations around the $x$-, $y$- and $z$-axes and symmetries with respect to the $xy$-, $yz$-, $zx$-planes.

Among them, we count the number of each type of local point configurations. Table 6 shows the result for each neighborhood system.

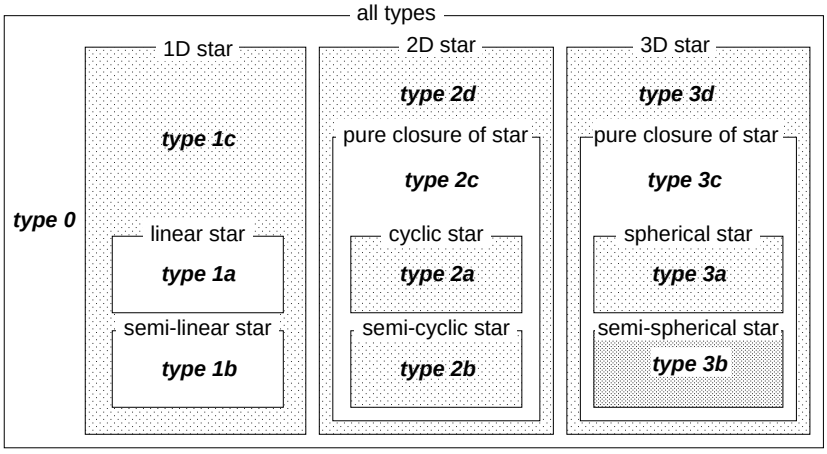


Fig. 13. Hierarchical point classification by topological characterization of stars in $\mathbb{Z}^3$.

Table 6
The numbers of different local point configurations in a $3 \times 3 \times 3$ region for each of the twelve types, with respect to the 6-, 18- and 26-neighborhood system, up to rotations and symmetries.

| | 6-neighborhood | 18-neighborhood | 26-neighborhood |
|---|---|---|---|
| **type 0** | 23 520 | 22 | 1 |
| **type 1a** | 200 712 | 520 | 11 |
| **type 1b** | 134 280 | 143 | 3 |
| **type 1c** | 103 092 | 735 | 77 |
| **type 2a** | 26 862 | 2 852 | 55 |
| **type 2b** | 345 016 | 18 741 | 398 |
| **type 2c** | 113 008 | 19 324 | 3 203 |
| **type 2d** | 399 329 | 18 434 | 3 664 |
| **type 3a** | 1 | 23 520 | 23 520 |
| **type 3b** | 14 031 | 345 997 | 290 979 |
| **type 3c** | 374 | 131 073 | 321 371 |
| **type 3d** | 65 919 | 864 783 | 782 862 |
| total | 1 426 144 | 1 426 144 | 1 426 144 |

As a matter of fact, the type of the central point $\boldsymbol{x}$ is not determined by $\mathbf{C}_m$, but by $star(\boldsymbol{x} : \mathbf{C}_m)$. Therefore, we do not need to observe all points in $Sk(\mathbf{C}_m)$ but only those in $Sk(Cl(star(\boldsymbol{x} : \mathbf{C}_m)))$ for obtaining the point type of $\boldsymbol{x}$. For example, Fig. 14 shows examples of two different 3-complexes $\mathbf{C}_6$ and $\mathbf{C}'_6$ whose central points have type 3b such that

$$Sk(\mathbf{C}_6) \neq Sk(\mathbf{C}'_6)$$

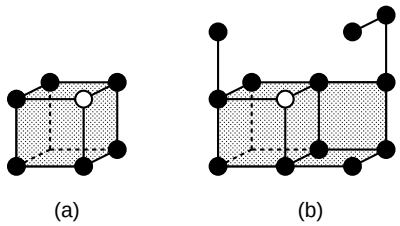


Fig. 14. Examples of two different 3-complexes $\mathbf{C}_6$ (a) and $\mathbf{C}'_6$ (b) whose central points, illustrated as white points, have type 3b such that $Sk(\mathbf{C}_6) \neq Sk(\mathbf{C}'_6)$ but $Sk(Cl(star(\boldsymbol{x} : \mathbf{C}_6))) = Sk(Cl(star(\boldsymbol{x} : \mathbf{C}'_6)))$.

Table 7
The numbers of star configurations for each of the twelve types, with respect to the 6-, 18- and 26-neighborhood system, up to rotations and symmetries.

| | 6-neighborhood | 18-neighborhood | 26-neighborhood |
|---|---|---|---|
| **type 0** | 1 | 1 | 1 |
| **type 1a** | 2 | 6 | 11 |
| **type 1b** | 1 | 2 | 3 |
| **type 1c** | 6 | 17 | 77 |
| **type 2a** | 6 | 80 | 55 |
| **type 2b** | 14 | 313 | 398 |
| **type 2c** | 123 | 938 | 3 203 |
| **type 2d** | 74 | 461 | 3 664 |
| **type 3a** | 1 | 21 425 | 23 520 |
| **type 3b** | 9 | 102 793 | 290 979 |
| **type 3c** | 11 | 58 532 | 321 371 |
| **type 3d** | 274 | 179 893 | 782 862 |
| total | 522 | 364 461 | 1 426 144 |

but

$$Sk(Cl(star(\boldsymbol{x} : \mathbf{C}_6))) = Sk(Cl(star(\boldsymbol{x} : \mathbf{C}'_6))). \tag{5}$$

Obviously, because of (5), they have the same type 3b, and have the same forms around the central points.

For $m = 6, 18$, the following equation does not always hold;

$$Sk(\mathbf{C}_m) = Sk(Cl(star(\boldsymbol{x} : \mathbf{C}_m))), \tag{6}$$

while it always holds for $m = 26$. For example, we see in Fig. 14 that (6) holds for $\mathbf{C}_6$ (a) but does not for $\mathbf{C}'_6$ (b). In order to avoid counting the local point configurations twice for $\mathbf{C}_6$ and $\mathbf{C}'_6$ in Fig. 14, we count different configurations of $Sk(Cl(star(\boldsymbol{x} : \mathbf{C}_m)))$ instead of those of $Sk(\mathbf{C}_m)$. Such configurations are called star configurations and we obtain Table 7. Note that $star(\boldsymbol{x} : \mathbf{C}_m)$ is not a discrete complex so that we make a smallest complex by using the closure function before taking its skeleton. We also mention that we count configurations of $star(\boldsymbol{x} : \mathbf{C}_m)$ up to rotations and symmetries; thus no redundant configuration is contained in Table 7.

Clearly, the number of star configurations for each type in Table 7 is smaller than that of local point configurations in Table 6 for $m = 6, 18$. We also see that the total numbers of different star configurations for $m = 6, 18$ are much smaller than that for $m = 26$.

Now let us also consider the cube decomposition of Table 4 for $m = 18$ to obtain the more precise results for Table 7. Experimentally, if we consider all possible cube decompositions such as Tables 3 and 4, the results for $m = 18$ in Table 7 become slightly bigger numbers for all the 2-dimensional stars and the types 3c and 3d: 88 for type 2a, 347 for type 2b, 1309 for type 2c, 558 for type 2d, 58890 for type 3c, and 184393 for type 3d. For the other stars including type 3b which is of our interest in this paper, the numbers of configurations become the same as those in Table 7. This is because, as far as the case of type 3b be concerned, influences on star configurations may be made by modification of polyhedral complexes in Fig. 4 when the central point $\boldsymbol{x}$ is considered to be the leftmost (or rightmost) point in Fig. 4, and such a modification seems not to change $Sk(Cl(star(\boldsymbol{x} : \mathbf{C}_{18})))$ even if it may change $\mathbf{C}_{18}$ itself.

## 5 Local configurations in discrete combinatorial surfaces

Our discrete combinatorial surfaces appear at the 2-dimensional combinatorial boundaries of 3-complexes, that is, $\partial\mathbf{C}$ where $dim(\mathbf{C}) = 3$. Because $star(\boldsymbol{x} : \partial\mathbf{C})$ is cyclic if $star(\boldsymbol{x} : \mathbf{C})$ is semi-spherical from Proposition 20, we see that semi-spherical stars whose point type is 3b give all local configurations appearing in such discrete combinatorial surfaces.

Let us consider a set of boundary points $Br_{m'}(\mathbf{V})$ of (1) for $m' = 6, 18, 26$. In [14], we see that $Br_{m'}(\mathbf{V})$ includes all types of points except for spherical points (type 3a) which are interior points of $\mathbf{V}$ and that there are relations between our discrete complexes $\mathbf{C}_m$ constructed from $\mathbf{V}$ and $Br_{m'}(\mathbf{V})$ only for the pairs $(m, m') = (6, 18), (6, 26), (18, 6), (26, 6)$ [14]. Those relations indicate that boundary points of $Br_{m'}(\mathbf{V})$ do not have always semi-spherical stars, but also the other stars such as one-, two- and three-dimensional stars except for spherical stars depending on their local point configurations. By using our topological classification of local point configurations in the previous section, we easily discriminate semi-spherical stars from the other stars on boundaries.

As shown in Table 7, the numbers of semi-spherical star configurations of $Sk(Cl(star(\boldsymbol{x} : \mathbf{C}_m)))$ are still large, especially for $m = 18, 26$. What we are interested in, however, is point configurations of stars of $\boldsymbol{x}$ in combinatorial boundaries $\partial\mathbf{C}_m$ but not in $\mathbf{C}_m$. For example, we have different discrete complexes $\mathbf{C}_m$ and $\mathbf{C}'_m$ such that $Sk(\mathbf{C}_m) \supset Sk(\mathbf{C}'_m)$ and $star(\boldsymbol{x} : \partial\mathbf{C}_m) = star(\boldsymbol{x} : \partial\mathbf{C}'_m)$ as illustrated in Fig. 15.

Table 8
The numbers of surface star configurations for the 6-, 18- and 26-neighborhood systems.

| | 6-neighborhood | 18-neighborhood | 26-neighborhood |
|---|---|---|---|
| # of surface stars | 6 | 1 412 | 6 028 |

Note that this does not occur for $m = 6$. However, we have the case that $\mathbf{C}_6 \neq \mathbf{C}'_6$ and $star(\boldsymbol{x} : \partial\mathbf{C}_6) = star(\boldsymbol{x} : \partial\mathbf{C}'_6)$ as shown in Fig. 16. We can also say that two discrete surfaces in Fig. 16 have the same shape but do not have the same orientation if we consider that they have two sides, the inside and outside.

In order to avoid counting twice for such two discrete complexes $\mathbf{C}_m$ and $\mathbf{C}'_m$ in Figs. 15, 16 respectively, we consider point configurations of $Sk(Cl(star(\boldsymbol{x} : \partial\mathbf{C}_m)))$ instead of those of $Sk(Cl(star(\boldsymbol{x} : \mathbf{C}_m)))$. Such point configurations are called surface star configurations. The results of counting different surface star configurations up to rotations and symmetries for $m = 6, 18, 26$ are shown in Table 8. For $m = 18$, we first calculate the result in Table 8 considering a unique complex for each local point set by using only Table 3 as mentioned before. If we consider all possible polyhedral complexes for each local point set, including the case of Fig. 4, we obtain 1720 instead of 1412 in Table 8. We verified that our results for $m = 6$ are the same as those in reference [8], which are illustrated in Fig. 2.

For $m = 6$, we see that surface star configurations are exactly the same as cyclic star configurations (type 2a in Table 7). However, for $m = 18, 26$, they

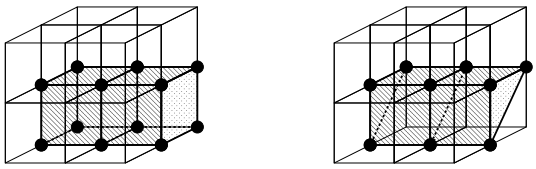

(a) (b)

Fig. 15. Two different discrete complexes $\mathbf{C}_{26}$ (a) and $\mathbf{C}'_{26}$ (b) around the central points $\boldsymbol{x}$ such that $star(\boldsymbol{x} : \partial\mathbf{C}_{26}) = star(\boldsymbol{x} : \partial\mathbf{C}'_{26})$.

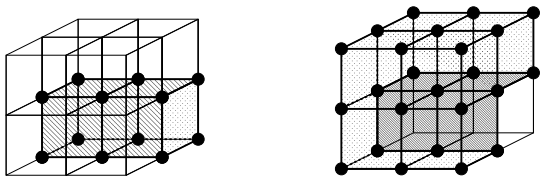

(a) (b)

Fig. 16. Two different discrete complexes $\mathbf{C}_6$ (a) and $\mathbf{C}'_6$ (b) around the central points $\boldsymbol{x}$ such that $star(\boldsymbol{x} : \partial\mathbf{C}_6) = star(\boldsymbol{x} : \partial\mathbf{C}'_6)$.

contain more configurations than cyclic star configurations. One of the reasons is that a cyclic star requires that both interior and exterior points which are separated by a discrete surface exist in $\mathbf{N}_{26}(\boldsymbol{x})$. For $m = 18, 26$, there are some surface star configurations where there is no interior point as illustrated in Fig. 1 (center).

## 6 Conclusions

Given a subset $\mathbf{V} \subseteq \mathbf{N}_{26}(\boldsymbol{x})$, we presented a method for classifying the central point $\boldsymbol{x}$ into one of the twelve types by the topological characterization of its star after obtaining a complex $\mathbf{C}_m$. Considering that boundary points having type 3b form discrete combinatorial surfaces as Proposition 20, we counted local configurations in discrete surfaces such as local point configurations whose central point has type 3b, namely $Sk(\mathbf{C}_m)$, and obtained 14031, 345997 and 290979 configurations for $m = 6, 18, 26$, respectively, up to rotations and symmetries. We also obtained 9, 102793 and 290979 semi-spherical star configurations, namely, $Sk(Cl(star(\boldsymbol{x} : \mathbf{C}_m)$, and 6, 1412 and 6028 surface star configurations, namely, $Sk(Cl(star(\boldsymbol{x} : \partial\mathbf{C}_m)))$, for $m = 6, 18, 26$, respectively. For $m = 18$, if we consider all possible polyhedral complexes $\mathbf{C}_{18}$ which may break the uniqueness of complex construction for certain local point sets $\mathbf{V}$ (but still keep the finiteness), we obtain 1720 surface star configurations. The same surface star configurations for $m = 6$ are already presented in reference [8] and they are illustrated in Fig. 2. We see that a boundary point illustrated as the central point in Fig. 1 (center) has a surface star configuration. This explains why our discrete surfaces have more configurations than

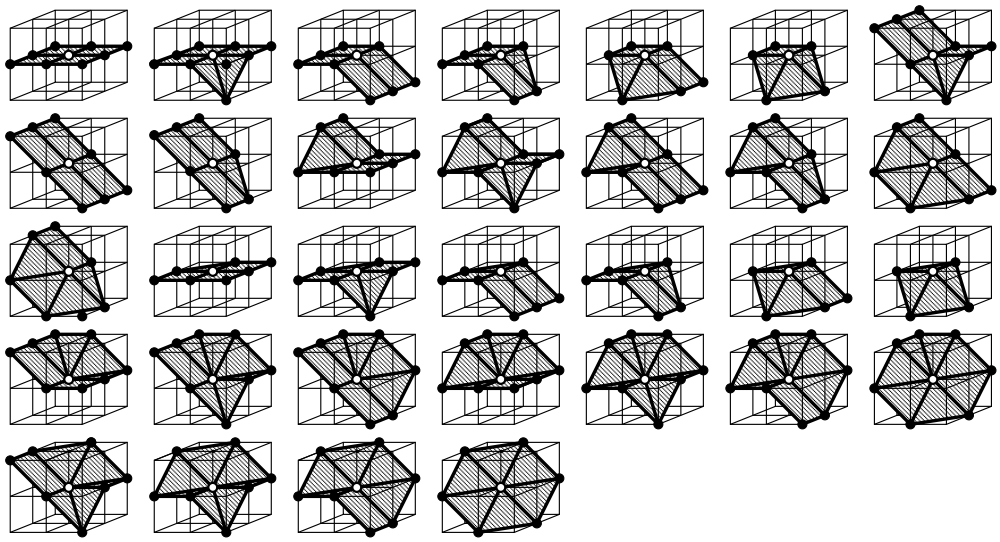

Fig. 17. The 32 local star configurations which appear in discrete combinatorial planes for the 26-neighborhood system.

that of simplicity surfaces [6].

References [9,13] show that there are 5 and 32 different configurations of stars which appear in discrete combinatorial planes for $m = 6, 26$, respectively. Such planar stars for $m = 6$ are shown as the five left configurations in Fig. 2. We also illustrate the 32 configurations of planar stars for $m = 26$ in Fig. 17. Note that oriented surfaces are considered in [9,13] so that 8 and 34 configurations are obtained for $m = 6, 26$. While there is only one non-planar star for $m = 6$, we see that, for $m = 26$, most of the 6028, namely 5994 surface stars are non-planar and they do not appear on discrete planes but appear on discrete non-planar surfaces. Figure 18 shows that, for example, every boundary point appearing at the faces of a digitized cube has one of the 32 planar stars illustrated in Fig. 17. On the other hand, around the vertices and edges of a digitized cube, boundary points have non-planar stars. Figure 18 also shows that many boundary points on non-planar surfaces such as a sphere, a one-sheet hyperboloid and a hyperbolic paraboloid have planar stars rather than non-planar stars. From such experiments, we consider that the study on local configurations of boundary points in the 26-neighborhood system might be useful for shape analysis of three-dimensional images. We remark that the

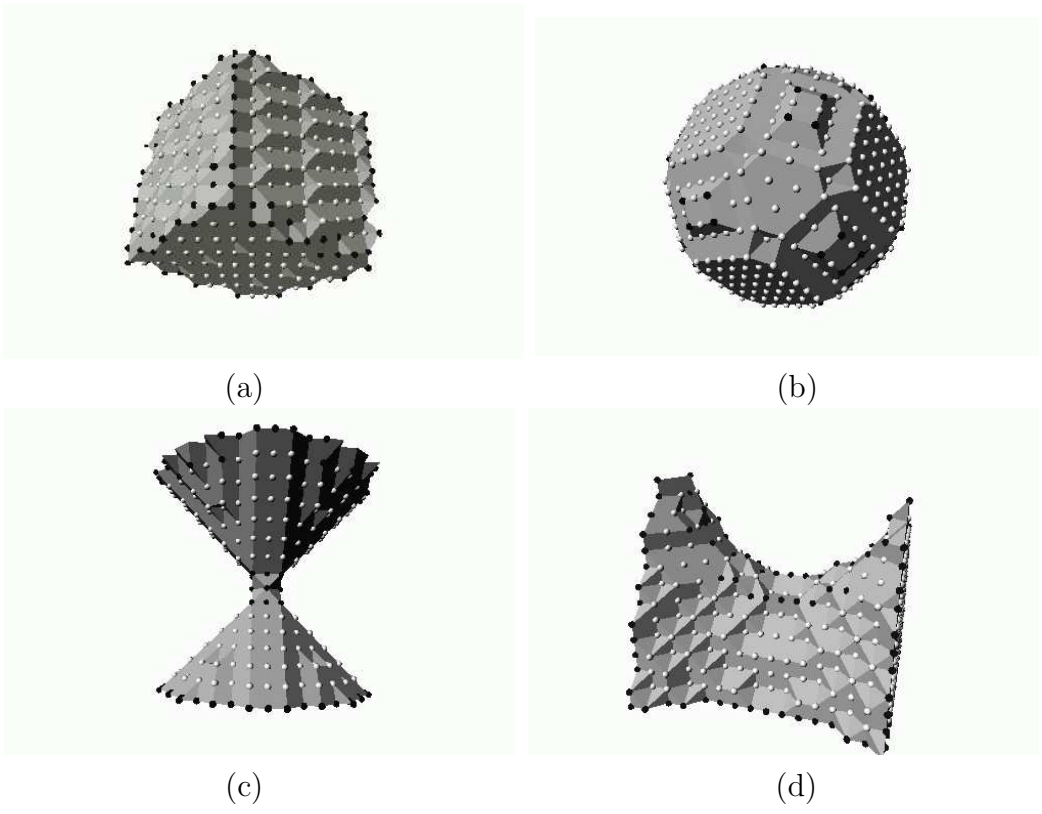


Fig. 18. Boundary points of three-dimensional digitized objects, such as a cube, a sphere, a one-sheet hyperboloid and a hyperbolic paraboloid, are classified into two types in the 26-neighborhood system: they are illustrated as white and black points if the stars are planar and non-planar, respectively.

similar shape analysis may work for $m = 18$ and may not be worth doing for $m = 6$ because most of all boundary points of three-dimensional digitized objects have planar stars as illustrated in Fig. 19.

**Acknowledgements.** A part of this work was supported by Grant-in-Aid for Scientific Research of the Ministry of Education, Culture, Sports, Science and Technology of Japan under the contract of 16650040 and was done under the research collaboration framework of National Institute of Informatics in Japan.

## References

[1] P. S. Alexandrov, *Combinatorial Topology*, Vol. 1, Graylock Press, Rochester, New York, 1956.

[2] G. Bertrand, "New notions for discrete topology," In LNCS 1568 : Discrete Geometry for Computer Imagery, Proceedings of 8th International Conference, DGCI'99, pp.218–228, Springer-Verlag, Berlin Heidelberg New York, 1999.

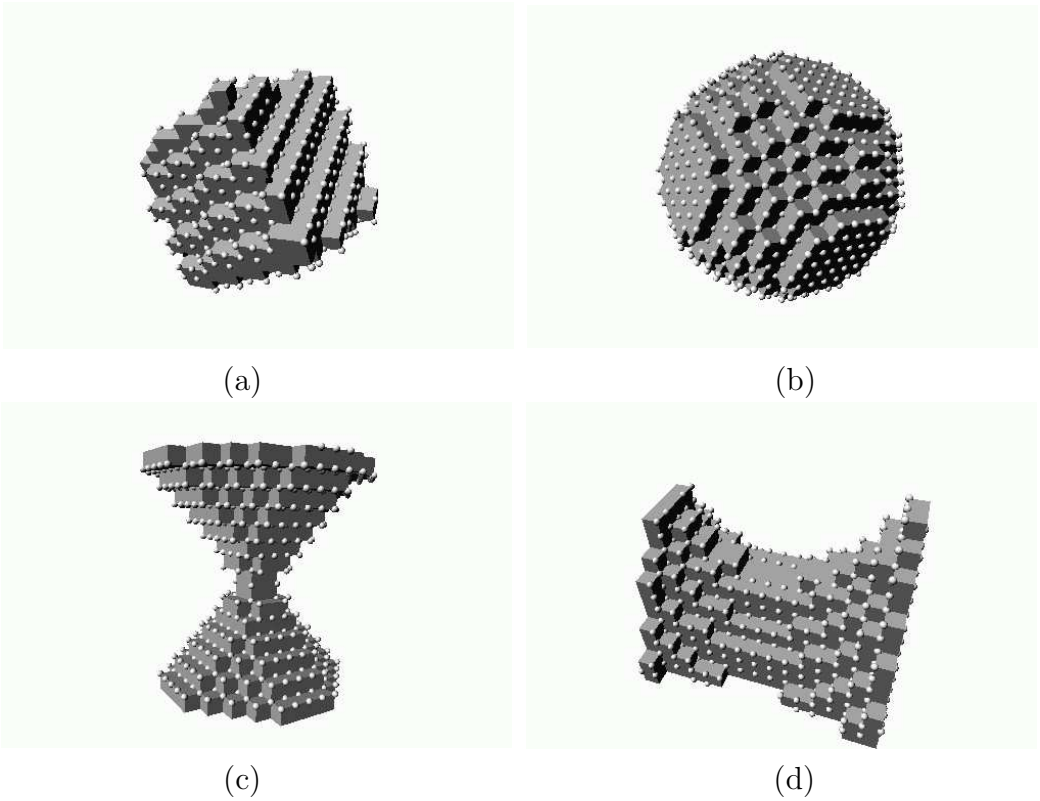


Fig. 19. Most boundary points of three-dimensional digitized objects, for example, a cube, a sphere, a one-sheet hyperboloid, and a hyperbolic paraboloid have planar surface stars illustrated as white points.

[3] G. Bertrand, M. Couprie, "A model for digital topology," In LNCS 1568 : Discrete Geometry for Computer Imagery, Proceedings of 8th International Conference, DGCI'99, pp.229–241, Springer-Verlag, Berlin Heidelberg New York, 1999.

[4] J. C. Ciria, A. de Miguel, E. Domínguez, A. R. Francés, A. Quintero, "Local characterization of a maximum set of digital $(26, 6)$-surfaces," In LNCS 3429 : Discrete Geometry for Computer Imagery, Proceedings of 12th International Conference, DGCI2005, pp.161-171, Springer-Verlag, Berlin Heidelberg, 2005.

[5] L. D. Cohen, "On active contour models and balloons," Computer Vision, Graphics and Image Processing: Image Understanding, Vol. 53, No. 2, pp. 211-218, 1991.

[6] M. Couprie, G. Bertrand, "Simplicity surface: a new definition of surfaces in $\mathbf{Z}^3$," In Vision Geometry VII, Proceedings of SPIE, Vol. 3454, pp. 40-51, 1998.

[7] A. Esnard, J-O. Lachaud, A. Vialard, "Discrete deformable boundaries for 3D image segmentation," Technical Report No. 1270-02, LaBRI, University of Bordeaux 1, 2002.

[8] J. Françon, "Discrete combinatorial surfaces," Graphical Models and Image Processing, Vol. 57, No. 1, pp. 20-26, 1995.

[9] J. Françon, "Sur la topologie d'un plan arithmétique," Theoretical Computer Science, Vol. 156, pp. 159-176, 1996.

[10] A. Imiya, U. Eckhardt, "The Euler characteristics of discrete objects and discrete quasi-objects," Computer Vision and Image Understanding, Vol. 75, No. 3, pp. 307-318, 1999.

[11] P. P. Jonker, S. Svensson, "The generation of N dimensional shape primitives," in LNCS 2886 : Discrete Geometry for Computer Imagery, Proceedings of 11th International Conference, DGCI2003, pp.420-433, Springer-Verlag, Heidelberg, 2003.

[12] Y. Kenmochi, A. Imiya, A. Ichikawa, "Discrete combinatorial geometry," Pattern Recognition, Vol. 30, No. 10, pp. 1719-1728, 1997.

[13] Y. Kenmochi, A. Imiya, "Combinatorial topologies for discrete planes", in LNCS 2886 : Discrete Geometry for Computer Imagery, Proceedings of 11th International Conference, DGCI2003, pp.144-153, Springer-Verlag, Heidelberg, 2003.

[14] Y. Kenmochi, A. Imiya, "Combinatorial boundary of a 3D lattice point set," to appear in Journal of Visual Communication and Image Representation.

[15] Y. Kenmochi, Y. Nomura, "Local point configurations of discrete combinatorial surfaces", in LNCS 3429 : Discrete Geometry for Computer Imagery, Proceedings of 12th International Conference, DGCI2005, pp. 336-347, Springer-Verlag, Heidelberg, 2005.

[16] E. Khalimsky, R. Kopperman, P. R. Meyer, "Computer graphics and connected topologies on finite ordered sets," Topology and its Applications, Vol. 36, pp. 1-17, July 1990.

[17] T. McInerney, D. Terzopoulos, "Deformable models in medical images analysis: a survey," Medical Image Analysis, Vol.1, No.2, pp. 91-108, 1996.

[18] D. G. Morgenthaler, A. Rosenfeld, "Surfaces in three-dimensional digital images," Information and Control, Vol. 51, pp. 227-247, 1981.

[19] J. Stillwell, *Classical Topology and Combinatorial Group Theory*, Springer, New York, 1993.

[20] G. M. Ziegler, *Lectures on Polytopes*, Springer, New York, 1998.